ELSEVIER

Journal of Photochemistry and Photobiology A: Chemistry 105 (1997) 269–276

Journal of PHOTOCHEMISTRY AND PHOTOBIOLOGY A:CHEMISTRY

Theoretical model of photoinduced intramolecular charge transfer processes

Pier Luigi Nordio *, Antonino Polimeno, Giacomo Saielli

Department of Physical Chemistry, University of Padova, Via Loredan 2, 35131 Padova, Italy

Received 8 August 1996; accepted 13 November 1996

Abstract

Molecular systems which undergo upon photoexcitation intramolecular charge transfer processes accompanied by conformational changes are known to exhibit complex spectroscopic and dynamical behaviour. Typical spectroscopic effects are dual fluorescence and pronounced solvatochromism. Dynamical features are revealed by the temperature dependence of fluorescence emission intensities and shifts under stationary conditions; the precursor–successor behaviour for the observed decay of the high-frequency band and the rise of the low-frequency band, after pulse excitation in correspondence of the high-frequency absorption; the fluorescence depolarization effects; the dynamic Stokes shifts measured in time-dependent experiments. All these effects can be rationalized by a stochastic model in which coupling of the fluorescent probe with the polar environment is explicitly taken in account. Ingredients of the model are the potential energy surface for the probe internal coordinates, and hydrodynamic and dielectric properties of the solvent. The model reduces to the simple kinetic scheme based on two-state interconversion process only in the limiting case of a relatively high energy barrier separating the two emitting states, and rapid equilibration of the polar solvent with respect to the instantaneous probe dipole moment. © 1997 Elsevier Science S.A.

Keywords: Internal charge transfer; Solvation effects; Stochastic model; Dual fluorescence

1. Introduction

When a probe molecule is dissolved in a liquid of normal viscosity and density it may undergo dynamical processes which bear no resemblance to those occurring in the gas phase. Thus its rotational behaviour will in general appear as diffusional, i.e., characterized by random sequences of small amplitude jumps, the angular momentum being effectively quenched by the frequent collisions with the surrounding solvent molecules. The collisions slow down the rotational motion with respect to the frequency typical for the inertial condition in the gas phase, introducing effective frictional drags. On the other hand, if rotations about specific bonds are hindered in the isolated molecule by energy barriers, molecular collisions generally provide the most important mechanism for promoting internal motions, by supplying the extra energy necessary to overcome the barrier [1]. This is certainly the case for the rotations of alkyl and amino groups, of benzene rings in biphenyl-like molecules, or of the larger groups involved in the photo-isomerization of stilbenes and 1,1′-binaphthyls. Unequivocal indication of dynamical effects determined by the solvent comes from the dependence upon solvent viscosity of the observed kinetic rates. Under these circumstances, many-body treatments are required for the understanding and the rationalization of the experiments. Molecular dynamics (MD) calculations may appear the main route to follow the time evolution of molecular systems undergoing conformational kinetics. Even if quantum description would be desirable, criteria based on the relative size of energy level spacings and average thermal energy can often justify the classical approach. The success of MD calculations for the isomerization dynamics of small molecules in the liquid state [2] supports the validity of the classical description. However, the heavy numerical procedures inherent to the MD method may sometimes prevent a simple physical insight on the relevant aspects of the system behaviour. According to this point of view, analytical methods based on stochastic equations, generally referred to as diffusion or Fokker–Planck equations, are undoubtedly preferable. Under suitable conditions, solutions of stochastic equations are formally equivalent to those provided by MD calculations, as it will be discussed in a next section.

Up to now, the solvent has been considered only as the provider of frequent impulsive interactions ('collisions') with random time distribution. When a dipolar molecule is dissolved in a polar environment, the specificity of the result-

* Corresponding author. Fax: +39-49-8275135.

PII S1010-6030(96)04569-8

ing interaction which adds to those giving rise to viscous frictional effects, has to be taken properly into account. This kind of interaction is responsible for a dielectric contribution to the friction acting on a rotating dipole [3], and for static and dynamic Stokes shifts observed in fluorescence spectra when the dipole moment of a fluorescent probe varies upon photoexcitation [4–6]. In this paper, we shall present theoretical simulations of spectroscopic experiments, performed on molecular systems which undergo, upon photoexcitation in polar solvents, an intramolecular charge transfer coupled to a structural change [7,8]. For sake of simplicity, a two-variable system, made of a solute internal degree of freedom and a single solvent collective coordinate, has been solved numerically. Even for such a simple model the computational effort is quite relevant. The theoretical tool for describing the system kinetics is provided by a bidimensional diffusion equation, which contains no freely adjustable parameters and can be solved exactly for all dynamical regimes. Other 'important' coordinates might be included at the cost of much heavier computational effort, but such an extension is not required to account for the experimental observations addressed in this paper. The agreement with different experimental outcomes is indeed surprisingly good, confirming that the important physical ingredients are contained in the model.

2. Photophysical systems

A number of calculations [9,10] has been made in the last few years by the Padova Theoretical Group to interpret the dynamical behaviour of donor–acceptor substituted benzene derivatives, i.e., dimethylaminobenzonitrile (DMABN) and related compounds, and the physical view emerging from the analysis will be reviewed in this paper. The most remarkable features exhibited by the fluorescence spectra of these systems are:

(1) The presence of two fluorescence bands centred at about 350 and 450 nm respectively, after excitation at the lowest wavelength in solvents of intermediate polarity.

(2) The pronounced solvatochromic effect [7]: in non-polar solvent only the high-frequency band is present, the low-frequency band appearing with increasing intensity in solvent of increasing polarity. A red shift of the band maximum, proportional to solvent polarity, is also observed.

(3) A characteristic temperature dependence of the ratio between the intensities of the high-frequency and low-frequency band in a given solvent [7]. This ratio goes through a maximum at about 200 K for solvents of intermediate polarity and viscosity.

(4) An analogous change with temperature of the polarization ratio $I_{\parallel}/I_{\perp}$ for the two bands, when polarized light is used as exciting source [11]. The low-frequency fluorescence is completely depolarized at about the same temperature at which the maximum in its intensity occurs, while high-frequency fluorescence is depolarized at much higher temperatures.

(5) The precursor-successor behaviour observed for the decay of the high-frequency band and the rise of the low-frequency band, after a laser pulse excitation in correspondence of the high-frequency absorption [12].

(6) A noticeable time-dependent Stokes shift which accompanies the rise of the low-frequency band, in pulse fluorescence experiments [13,14].

The hypothesis of a transient intramolecular charge transfer in the first electronically excited state of the molecule was first introduced by Grabowski et al. [15] to explain the observed dual fluorescence. Two metastable states with different emission intensity were assumed to exist: a planar locally excited (LE) state directly reached from the ground state upon pulse excitation, which subsequently converts within its lifetime into a twisted charge transfer (CT) state, stabilized by polar solvents. The reversible conformational change was consider to be a 90°-twist of the dimethylamino group out of the benzene ring plane, even if rehybridization of the amino nitrogen bond orbitals should also be considered [16]. The Grabowski kinetic scheme, which considers the interconversion between LE and CT states, and their decay to the ground state by both radiative and non-radiative mechanisms, is able to give a qualitative interpretation of most effects related to the dual fluorescence phenomenon, but it overlooks the dynamic role played by the solvent. Besides, it is a phenomenological treatment, which provides no interpretation for the kinetic terms involved in the model.

3. The theoretical model

The theoretical model is based on a bidimensional diffusion equation on the coordinate pair (θ,X), where θ refers to the probe internal coordinate and X to a collective coordinate describing the reaction field exerted by the polar solvent. In order to have a clear understanding of the approximations inherent to the model and its limits of validity, one should recognize that in principle the diffusion equation can be derived from the many-body Newtonian equation of motion for the entire system (probe plus solvent molecules), under assumption of timescale separation. In other words, the characteristic time τ_R for the internal motion and the relaxation time τ_S for the spontaneous local polarity fluctuation are considered to be longer than the characteristic time for any other motional process occurring in the system, such as fluctuations of intermolecular interactions described by Lennard–Jones type potentials (responsible for viscous drags), and probe angular momentum relaxation. Analysis of experimental far infrared (fir) absorptions in polar liquids [17] shows indeed that the instantaneous cages in which dipole probes can undergo librations in the fir frequency regime (ca. $10^{13}\,s^{-1}$) have a lifetime of the order of 1 ps or less, and that within this time effective quenching of angular momenta actually occurs. Thus, the assumption of timescale separation can be reasonably adopted, the time constant for internal kinetics and solvent relaxation being of the order of 10–100 ps at

room temperature, and still longer at lower temperatures. The most crucial approximation remains the assumption of a single time constant for solvent relaxation, a distribution of times certainly appearing more reasonable on physical ground. If the approximations discussed above are valid, then the resulting diffusion equation is expected to give the same results of a full MD calculation on the same system. The diffusion equation is also formally analogous to a bidimensional Langevin equation, i.e., to an equation of motion for the (θ,X) variables in which damping factors are included. The diffusion equation provides the time evolution for the distribution $P(\theta,X,t)$, given appropriate initial conditions, and has the form [9,10]:

$$\frac{\partial}{\partial t}P(\theta,X,t)=\left[D_R\frac{\partial}{\partial\theta}\left(\frac{\partial}{k_BT}\frac{\partial E_1}{\partial\theta}+\frac{\partial}{\partial\theta}\right)+D_S\frac{\partial}{\partial X}\left(\frac{1}{k_BT}\frac{\partial E_1}{\partial X}+\frac{\partial}{\partial X}\right)\right]P(\theta,X,t) \quad (1)$$

where $E_1(\theta,X)$ is the potential energy function for the solute in the first excited state S_1 interacting with solvent, and D_R, D_S are diffusion coefficient for the θ and X variables, as defined below. The total energy for the solute–solvent system, when the fluorescent probe is in the ground state S_0 or in the excited state S_1 is:

$$E_{0,1}(\theta,X)=V_{0,1}(\theta)-\frac{1}{2\Xi_\infty^2}\mu_{0,1}(\theta)^2-\mu_{0,1}(\theta)X+\frac{1}{2}\Xi^2X^2 \quad (2)$$

where $V_{0,1}(\theta)$ expresses the dependence upon the internal coordinate of the potential energy of the isolated probe molecule in S_0 and S_1 state, respectively, and $\mu_{0,1}(\theta)$ are the corresponding dipole moments. The quantities Ξ and Ξ_∞ are functions of the static and optical dielectric constants [18]:

$$\frac{1}{\Xi^2}=\frac{1}{\Xi_0^2}-\frac{1}{\Xi_\infty^2}=\frac{1}{V}\left(\frac{\epsilon_0-1}{\epsilon_0+1/2}-\frac{\epsilon_\infty-1}{\epsilon_\infty+1/2}\right) \quad (3)$$

where V is the volume of the Onsager cavity. The third-term at the rhs of Eq. (2) represents the dipolar interaction between the instantaneous dipole moment of the fluorescent probe at the configuration defined by the internal coordinate θ, and the solvent reaction field. The correction to the gas-phase potential resulting from the electrostatic interaction with the solvent is completely attributed to this term.

The second term accounts for the fact that only the orientation polarization, and not the electronic term, contributes to dissipative mechanisms [18], while the last term provides a potential term which confines the amplitude of the spontaneous fluctuations of the solvent polarization. In the normal cases of rigid probes, polarization fluctuations cause dielectric friction effect on the probe reorientation, and dynamic Stokes shifts in time resolved fluorescence spectra when the dipole moment of the fluorescent state is different from that of the ground state, with which the surrounding solvent was at thermal equilibrium prior to the exciting pulse. The intrinsic relation between dielectric friction and Stokes shift effect is put into evidence in a paper by van der Zwan and Hynes [18].

It is interesting to look at the solutions of the diffusion equation in absence of coupling between the two variables. The solution for the X-dependent diffusion equation is analytical, and the decay of the polarization fluctuations is given by the correlation function:

$$\langle X(0)X(t)\rangle=\frac{k_BT}{\Xi^2}\exp\left(-\frac{D_S\Xi^2}{k_BT}t\right) \quad (4)$$

The pre-exponential factor corresponds to the mean-square amplitude of the fluctuations, and the time constant in the exponential defines the solvent fluctuation relaxation time:

$$\frac{k_BT}{\Xi^2}=\langle X^2\rangle \quad (5)$$

$$\frac{D_S\Xi^2}{k_BT}=\frac{1}{\tau_S} \quad (6)$$

The solution for the θ-dependent diffusion equation cannot be recovered in closed form in the presence of a potential term $V(\theta)$. However, if $V(\theta)$ exhibits two minima separated by a relatively high barrier ($\Delta/k_BT>1$), a reliable approximation to the rate constant for the passage across the barrier can be obtained by using the formula derived by Kramers [1] in its fundamental treatment of activated processes:

$$k=D_R\frac{V''(m)V''(M)}{2\pi k_BT}\exp(-\Delta/k_BT) \quad (7)$$

where $V''(m)$ and $V''(M)$ denote potential curvatures at the starting minimum and at the top of the barrier, respectively. In this case, $D_R=1/\tau_R$ defines the characteristic time for the internal motions, and Eq. (7) simply states that a slow down of the motion will occur in the presence of the potential barrier according to a Arrhenius type behaviour, as expected. The coupling of the molecular dipole with the local reaction field determined by the solvent polarization fluctuations changes the time behaviour of both the conformational process and the solvent relaxation. It is therefore necessary to resort to numerical solutions of the diffusional problem. The algorithms employed are described elsewhere [9]; it will suffice here to note that diffusion equation are second-order differential equations similar to the quantum-mechanical Schrodinger equations, and after separation of the time variable they can be solved in a similar way by standard matrix algebra.

4. Parameterisation of the model

In order to simulate the fluorescence emission spectra under common experimental conditions, source and sink terms have to be included in the equation for the time evolution of $P(\theta,X,t)$. The source term responsible for the radiative pumping from the ground state has the form $S(\theta,X)T(t)$

and it allows to select both the energy surface region in which the excitation is produced, and to simulate different pulse shapes in time. In general, $S(\theta,X)$ is taken as a function peaked at $\theta=0$, multiplied by the Gaussian distribution for the solvent coordinate, corresponding to equilibrium with respect to the dipole moment of the probe in its ground state. The simplest choice for the pulse shape is that of an instantaneous pulse of unit intensity. The sink term is expressed by non-radiative decay of time constant of about 5 ns, the same for both bands as suggested by experimental findings. All physical parameters entering the theory are taken from experimental data or evaluated from well-established physical models:

(1) The dielectric constant values ϵ_0 and ϵ_∞ and their temperature dependence, are taken from the literature [19].

(2) The solvent relaxation time τ_S is related to the experimental dielectric relaxation time τ_D by the classical Onsager relation [18]

$$\frac{1}{\tau_S}=\frac{2\epsilon_0+1}{2\epsilon_\infty+1}\tau_D \tag{8}$$

(3) The correlation time τ_R for the internal motion and the solvent dielectric relaxation time τ_D are estimated by the Stokes–Einstein equation, in terms of size of the rotating groups and solvent viscosity η. The same equation is used to calculate the temperature dependence of internal motion and solvent relaxation time [9]:

$$\frac{1}{\tau_R}=\frac{k_BT}{8\pi\eta b^3}, \qquad \frac{1}{\tau_D}=\frac{k_BT}{4\pi\eta a^3} \tag{9}$$

(4) The dependence of the potential function $V_{0,1}(\theta)$ upon internal coordinate is taken from quantum-mechanical calculations reported in the literature [20].

(5) The dependence upon the internal coordinate of the permanent dipole moment of the fluorescent probe is taken as:

$$\mu_1(\theta)=\mu_{LE}+(\mu_{CT}-\mu_{LE})\sin^2(\theta) \tag{10}$$

In this way, the LE minimum is defined in the (θ,X) space by the point of coordinates $(0,\mu_{LE}/\Xi^2)$, while the CT minimum is located at $(\pi/2,\mu_{CT}/\Xi^2)$. The stabilization energies in polar solvents are then $E_{LE}^{solv}=\mu_{LE}^2/2\Xi_0^2$ and $E_{CT}^{solv}=\mu_{CT}^2/2\Xi_0^2$ for the two probe configurations, as expected. Potential energy surfaces relative to S_0 and S_1 states are displayed in Fig. 1. With these ingredients, fluorescence emission spectra are calculated by the function [21]

$$I_f(\omega,t)=\omega^3\int_0^\pi d\theta\int_{-\infty}^{\infty}dX\mu_e(\theta)P(\theta,X,t)g(\omega-\omega_0(\theta,X)) \tag{11}$$

where $g(\omega-\omega_0(\theta,X))$ is a band shape function centred at the emission frequency:

$$\omega_0(\theta,X)=[E_1(\theta,X)-E_0(\theta,X)]/\hbar \tag{12}$$

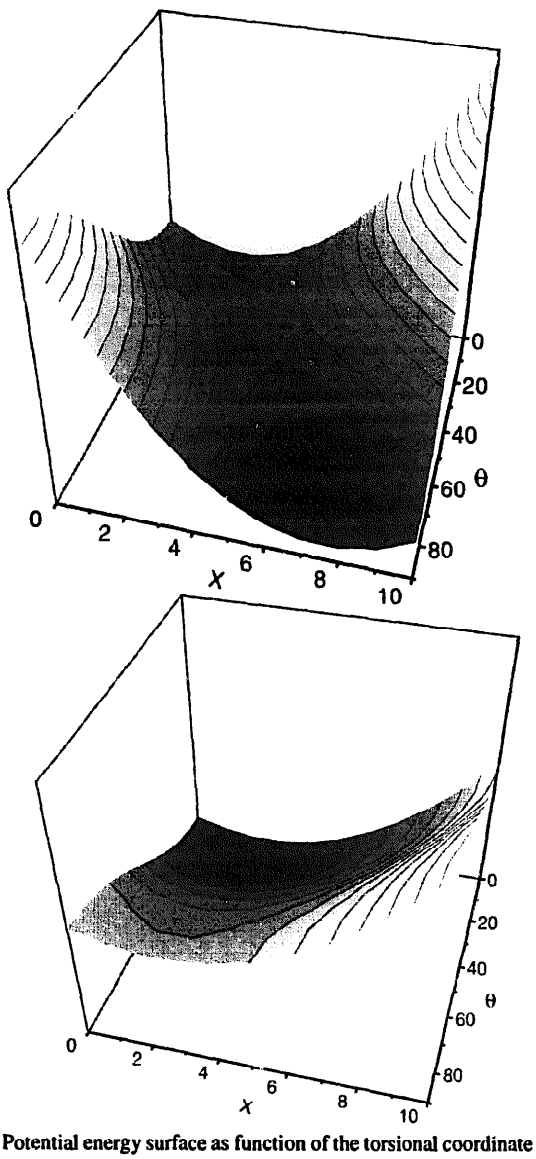

Fig. 1. Potential energy surface as function of the torsional coordinate θ and the solvent polarisation coordinate X, for DMABN in a solvent of intermediate polarity. Bottom: ground state S_0. Top: excited state S_1. The potential barrier separating LE ($\theta=0$) from CT ($\theta=\pi/2$) is of the order of 1 k_BT unit at normal temperatures.

chosen in such a way to reproduce the spectrum in non-polar solvents. In the integrand, $\mu_e(\theta)$ represents the transition dipole moment, which is assumed to have the functional form:

$$\mu_e(\theta)=a_0+a_1\cos^2(\theta) \tag{13}$$

with $a_1>a_0$. According to this expression, the transition is allowed for the planar configuration, but strictly forbidden for the twisted configuration if $a_0=0$. The correction term a_0 appears to be important in systems like piperidine (PIPBN) derivatives, where pre-twisting effects cannot be ruled out. By means of Eq. (11), fluorescence spectra can be simulated both for stationary conditions or after application of pulses of arbitrary shape.

5. Results

The main results obtained from the theoretical model are displayed in Figs. 2–6. Fig. 2 shows spectra simulated for

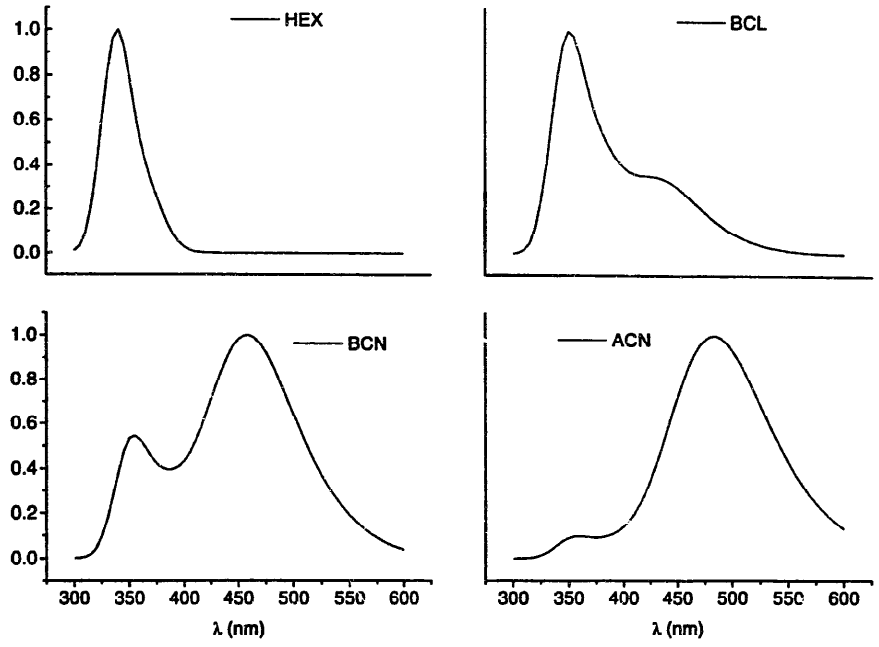

Fig. 2. Dual fluorescence predicted for DMABN in different solvents at room temperature. HEX: hexane; BCL: *n*-butylchloride; BCN: *n*-butyronitrile; ACN: acetonitrile.

different solvents at room temperature, and they compare well, both in the maximum positions and relative intensities of the two bands, with real experiments. The same is true for the temperature dependence of the fluorescent emission of DMABN in *n*-butyl chloride, shown in Fig. 3. The emission profile exhibits a minimum for the LE band, as a consequence of the opposite reactions occurring within the lifetime of the fluorescent state. Note, that in general the band intensities in the dual fluorescence spectrum do not reflect thermodynamic equilibrium, but rather the stationary condition which is attained during the lifetime of the excited state. Since only the LE state is directly excited by light absorption, at the lowest temperatures LE emission prevails because the rate constant for the LE → CT interconversion process is smaller than the rate for the LE decay to the ground state. At higher temperatures, the rate for the internal kinetics increases while

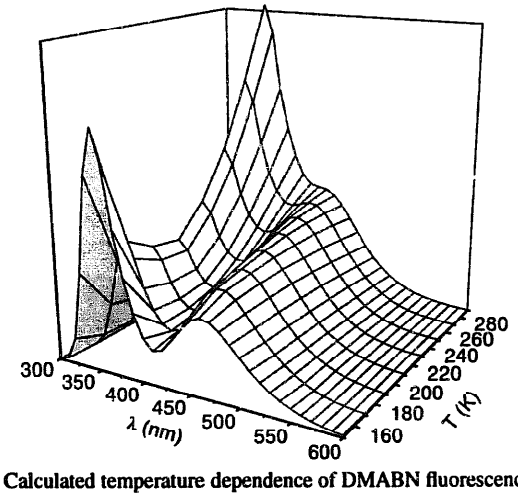

Fig. 3. Calculated temperature dependence of DMABN fluorescence emission spectra in *n*-butylchloride.

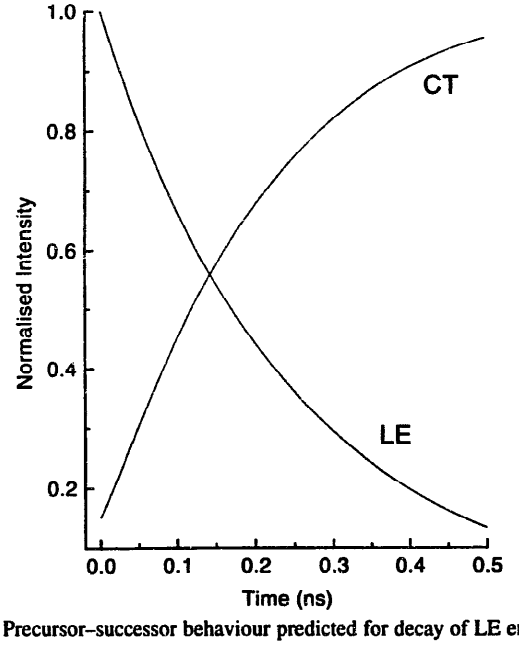

Fig. 4. Precursor–successor behaviour predicted for decay of LE emission at 350 nm and rise of CT emission at 450 nm, for DMABN in *n*-butylchloride at 173 K, after stepwise excitation at 350 nm. Decay of both signals due to the intrinsic lifetime of the S_1 state (ca. 5 ns) is almost ineffective in the timescale of the kinetic process.

the decay rate to ground state remains practically constant, and so the LE state is efficiently depopulated; but at still higher temperatures the rate for the inverse CT → LE process becomes eventually comparable to the decay rate, so that CT population is converted back to LE.

The precursor–successor behaviour predicted for DMABN in n-butyl chloride at 173 K, at the fixed wavelengths of 350 and 450 nm corresponding to LE and CT emission, is reported in Fig. 4. A stepwise excitation at 350 nm has been assumed

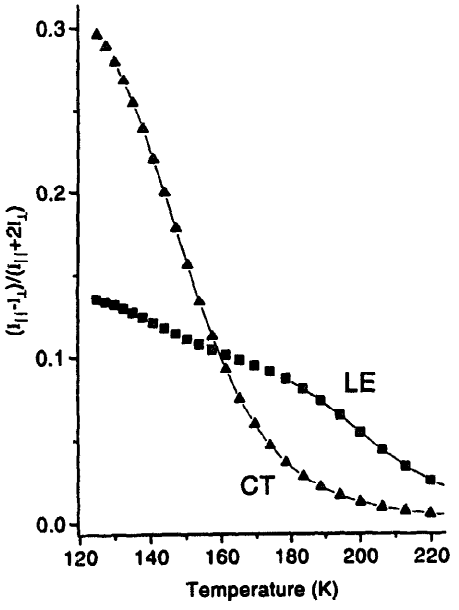

Fig. 5. Temperature dependence of fluorescence depolarisation simulated for the emission bands of DMABN in *n*-butylchloride/2-methylbutane mixtures. The CT band exhibit 'normal' behaviour, depolarisation occurring because of probe reorientation during the state lifetime of 5 ns. Up to 200 K, LE depolarisation does not occur, because rotational motions are practically frozen within the effective lifetime of the LE state, determined by the fast conversion to CT.

in the calculation. The temperature dependence of the depolarisation ratio $r(T)=(I_{\parallel}-I_{\perp})/(I_{\parallel}+2I_{\perp})$, calculated for the two emission bands of DMABN in the 9:1 mixture *n*-butylchloride/2-methylbutane [11], is given in Fig. 5. In this case, the rotational motion of the fluorescent probe was considered in the framework of a simplified kinetic scheme, in which the temperature dependence of kinetics rates and viscosities were taken into account. The solvent coordinate was not explicitly introduced because solvent relaxation was assumed to be always faster than other relevant processes, so that thermodynamic equilibrium could be assumed for local solvent polarisation. The behaviour reported in the figure is reminiscent of the temperature dependence of the LE/CT intensity ratio discussed above, and it is understood by realizing that in the explored temperature range the time window for an effective depolarisation mechanism is the intrinsic lifetime (5 ns) for the CT state, but the much shorter kinetic time constant for the LE state, undergoing fast conversion to CT. It follows that rotational motions can depolarise only the CT band, by considering that rotational motions of the whole probe molecule are somewhat slower than internal rotations, due to the larger size of the rotating moieties. Depolarisation of the LE band occurs at high temperature through an indirect mechanism, when the rate for the return process CT → LE is high enough to transfer into the LE state molecules which have lost orientational correlation with the initial photoselection.

Finally, a contour plot showing decay of the LE band, rise of the CT band and the time-dependent Stokes shifts relative to the latter emission is given in Fig. 6. The decay of the LE

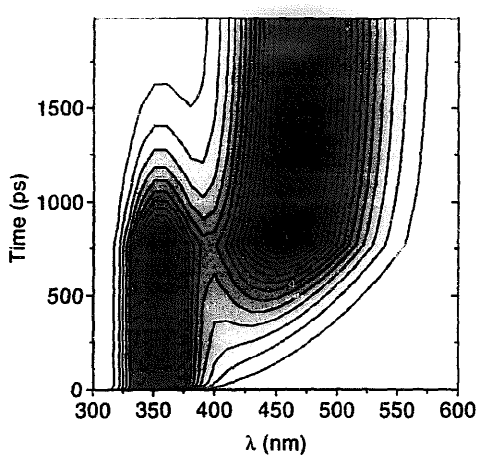

Fig. 6. Contour plot showing time evolution of band intensities calculated for PYRBN in GTA. A few hundreds ps after the excitation pulse the CT band is relatively intense, its maximum exhibiting a marked red-shift.

band and the subsequent rise of the CT emission intensity, denoted by the colour intensity, are clearly visible, as well as the red shift in time of the CT band maximum. The calculation refers to the physical case of pyrrolidine–benzonitrile (PYRBN) in glycerol triacetate (GTA), the time constant for interconversion being of the order of 250 ps and the transient Stokes shift characteristic time of about 600 ps.

The comparison of experiments and theoretical results provides convincing proof that the stochastic model is able to reproduce all relevant physical features of ICT processes. In particular, it confirms the widely accepted view of a thermally driven, reversible interconversion process occurring in the excited state of the DMABN molecules. When it is applied to real systems with the aim of simulating particular experimental data, some difficulty may actually arise, partly because important physical information on potentials surfaces, or dielectric and hydrodynamic properties, may not be available, and partly because of some simplifications inherent to the theory. The most crucial point is certainly the continuum model used to describe the polar environment, as revealed by subpicosecond fluorescence experiments on dye molecules [6]. Inclusion of additional internal coordinates, to account for rehybridization [16] or inertial effects, could be done in the framework of the model, at the cost of increased computational complexity. On the basis of recent results [22], however, inclusion of inertial coordinates are not expected to cause any dramatic change in the internal kinetics, at least for a reasonable choice of the model parameters.

Reference to other theoretical analysis dealing with the ICT process [23–25] in DMABN has been made elsewhere [9]. The main feature of the treatment discussed here resides on the fact that all energetic and dissipative effects are consistently taken into account within the framework of the model, and exact numerical solutions are performed. The important benefit obtained by the numerically exact solution of the dynamical problem, once that the physical ingredients are put into the model, is the direct insight of the system behaviour, when this becomes inherently complex because

of concurrence of different processes. Knowledge of the multidimensional energy surface, exhibiting relative minima associated with metastable states, and local maxima corresponding to saddle points, is an important prerequisite for dynamical calculations, but this information alone is of little help for predicting actual kinetic pathways. The time evolution of the system will be dictated by the condition of minimizing not only energy costs, but also frictional effects. Thus, each coordinate must be characterised by its own characteristic time; if this is long, motion along this coordinate will be slow, and eventually it will become the bottleneck for the overall process.

As a conclusion, the standard Kramers theory will be in general inadequate in the case of multidimensional systems characterised by different timescales [26]. In the bidimensional problem (θ,X) discussed here, the rate-determining step will be the torsional motion or the solvent relaxation, according to nature of the solvent, existence of an internal barrier and strength of the coupling. If the solvent is 'slow', it cannot equilibrate with the probe dipole moment in the instantaneous CT configuration originating from LE conversion, and dynamic Stokes shift will be observed [27]. In the limiting case of fast solvent relaxation, the Kramers formula can be applied if an effective torsional potential is defined by suitable averages of the starting dynamical equations over the fast variable [9]. However, validity of the Grabowski scheme should not be taken for granted because the particular form of the effective potential $V_{\mathrm{eff}}(\theta)$ [proportional to the logarithm of the reduced distribution $P(\theta)$, i.e., the average of the Boltzmann distribution of the excited state, $P(\theta,X)$, with respect to the fast solvent variable X], may imply multiexponential behaviour. The Grabowski kinetic equations are intrinsically unable to reproduce the resulting complex dynamics. The additional condition of well defined minima in correspondence of LE and CT states, separated by an energy barrier, is required.

To conclude, one may inquire if the theoretical results reported here can answer the controversial question about the nature of the internal coordinate involved in the CT process. As already mentioned, rehybridization of the nitrogen atom, rather than twisting of the amino group, has been associated by some authors to the charge transfer process [16].

The model discussed here is explicitly based on the original hypothesis of a twisted intramolecular charge transfer. Even if the theoretical predictions are in good agreement with experiment, it is unsafe to consider this result to be firm proof for the TICT model, for a number of reasons. First, it is reasonable to think, in the absence of reliable quantum-mechanical calculations, that the interplay of an internal potential $V(\theta_{\mathrm{h}})$ defined for the isolated molecule in term of a hybridization coordinate θ_{h}, with the solvent polarization effects, could not qualitatively alter the potential surface (shown in Fig. 1). Similarly, the phenomenological expression for $\mu_1(\theta)$ given in Eq. (10) would remain the same. Furthermore, the Stokes–Einstein relation is not accurate enough to distinguish between twisting and bending motions of the dimethylamino group. To summarize, it appears that most physical ingredients entering the dynamical model are rather insensitive to the detailed nature of the internal coordinate.

There is, however, a feature worth to be explored. The TICT model implies that LE emission is allowed, while CT emission at the $\theta=90°$ configuration is strictly forbidden for symmetry reasons. This is confirmed by quantum yield measurements [7,28], and explicitly considered in Eq. (11) and Eq. (13) to simulate the fluorescence experiments. There is, however, no a priori reason for such a difference in the emission intensity to be maintained, when considering molecular structures differing only for the amino nitrogen hybridization.

Acknowledgements

This work was supported by the Italian Ministry for Universities and Scientific and Technological Research, and in part by the National Research Council through its Centro Studi sugli Stati Molecolari, the Committee for Information Science and Technology, and the HCM contract No. ERBCHRXCT930282.

References

[1] H.A. Kramers, Physica 7 (1940) 284.
[2] R.W. Pastor and M. Karplus, J. Chem. Phys. 91 (1989) 211.
[3] T.W. Nee and R. Zwanzig, J. Chem. Phys. 52 (1970) 6353.
[4] M. Maroncelli and G.R. Fleming, J. Chem. Phys. 86 (1987) 6221.
[5] S. Kinoshita and N. Nishi, J. Chem. Phys. 89 (1988) 6612.
[6] M.A. Kahlow, T.J. Kang and P.F. Barbara, J. Chem. Phys. 88 (1988) 2372.
[7] E. Lippert, W. Rettig, V. Bonačić-Kouteký, F. Heisel and J.A. Miehé, Adv. Chem. Phys. 68 (1987) 1.
[8] W. Rettig, Topics Current Chem. 169 (1994) 254.
[9] G.J. Moro, P.L. Nordio and A. Polimeno, Mol. Phys. 68 (1989) 1131; A. Barbon, P.L. Nordio and A. Polimeno, Mol. Cryst. Liq. Cryst. 234 (1993) 69; A. Polimeno, A. Barbon, P.L. Nordio and W. Rettig, J. Phys. Chem. 98 (1994) 12158.
[10] D. Braun, P.L. Nordio, A. Polimeno and G. Saielli, Chem. Phys. 208 (1996) 127; G. Saielli, D. Braun, A. Polimeno and P.L. Nordio, Chem. Phys. Lett. 257 (1996) 381.
[11] A. Barbon, P. Lettinga and P.L. Nordio, Chem. Phys. 200 (1995) 41.
[12] W. Rettig, M. Vogel, E. Lippert and H. Otto, Chem. Phys. 103 (1986) 381.
[13] D. Braun, PhD Thesis, Humboldt Univ. Berlin, Koster Verlag, Berlin, 1995.
[14] G. Saielli, M. Ricci, P. Bartolini, R. Righini, A. Polimeno and P.L. Nordio, in preparation.
[15] Z.R. Grabowski, K. Rotkiewicz, A. Simiarczuk, D.J. Cowley and W. Baumann, Nouv. J. Chim. 3 (1979) 443.
[16] W. Schuddeboom, S.A. Jonker, J.M. Warman, U. Leinhos, W. Kühnle and K.A. Zachariasse, J. Phys. Chem. 96 (1992) 10809; T. von der Haar, A. Hebecker, Y. Il'ichev, Yun-Bao Jiang, W. Kühnle and K.A. Zachariasse, Recl. Trav. Chim. Pays-Bas 114 (1995) 430.
[17] P.L. Nordio and A. Polimeno, Chem. Phys. 180 (1994) 109.
[18] G. van der Zwan and J.T. Hynes, J. Phys. Chem. 89 (1985) 4181.
[19] A.M. Ras and P. Bordewijk, Rec. Trav. Chim. 90 (1971) 1055.
[20] S. Kato and Y. Amatatsu, J. Chem. Phys. 92 (1990) 7241.

[21] T.J. Kang, W. Jarzeba, P.F. Barbara and T. Fonseca, Chem. Phys. 149 (1990) 81.
[22] P.L. Nordio and A. Polimeno, Chem. Phys. 180 (1994) 109; P.L. Nordio and A. Polimeno, Int. J. Quantum Chem. 60 (1996) 321.
[23] T. Fonseca, H.J. Kim and J.T. Hynes, J. Molec. Liq. 60 (1994) 161.
[24] G.K. Schenter and C.B. Duke, Chem. Phys. Lett. 176 (1991) 563.
[25] S.G. Su and J.D. Simon, J. Chem. Phys. 89 (1988) 908.
[26] G. Moro, P.L. Nordio and A. Polimenom Chem. Phys. Lett. 182 (1991) 575; P.L. Nordio and A. Polimeno, Mol. Phys. 75 (1992) 1203; A. Polimeno and P.L. Nordio, Chem. Phys. Lett. 192 (1992) 509.
[27] P.L. Nordio and A. Polimeno, Mol. Phys. 88 (1996) 315.
[28] W. Rettig, Angew. Chem. Int. Ed. Engl. 25 (1986) 871.